

Atomistic calculations of ion implantation in Si: Point defect and transient enhanced diffusion phenomena

M. Jaraiz,^{a)} G. H. Gilmer, and J. M. Poate
AT&T Bell Laboratories, Murray Hill, New Jersey 07974

T. D. de la Rubia
Lawrence Livermore National Laboratory, Livermore, California 94550

(Received 29 September 1995; accepted for publication 7 November 1995)

A new atomistic approach to Si device process simulation is presented. It is based on a Monte Carlo diffusion code coupled to a binary collision program. Besides diffusion, the simulation includes recombination of vacancies and interstitials, clustering and re-emission from the clusters, and trapping of interstitials. We discuss the simulation of a typical room-temperature implant at 40 keV, $5 \times 10^{13} \text{ cm}^{-2}$ Si into (001)Si, followed by a high temperature (815 °C) anneal. The damage evolves into an excess of interstitials in the form of extended defects and with a total number close to the implanted dose. This result explains the success of the “+1” model, used to simulate transient diffusion of dopants after ion implantation. It is also in agreement with recent transmission electron microscopy observations of the number of interstitials stored in (311) defects. © 1996 American Institute of Physics. [S0003-6951(96)02803-1]

The transient enhanced diffusion (TED) of dopants in Si devices after ion implantation and annealing is proving to be a limiting factor in the scaling down of device sizes. This phenomenon is understood to result from excess interstitials, produced in the implant, interacting with dopants such as boron. In the continuum process simulators^{1,2} the Si interstitial excess is assumed to equal the implanted dose, the “+1” model.³ Accurate process modeling requires an understanding of the dominant mechanisms governing ion implantation and annealing. There are many fundamental questions regarding the collision cascade and resulting defect formation. In this work we show that atomistic modeling calculations can be used to quantitatively understand many aspects of the implant story. A key experimental contribution of this TED problem has been the recent discovery⁴, that, under appropriate conditions, the Si interstitials causing TED are emitted from rodlike (311) defects. This allowed the number of Si interstitials stored, and released, from these defects to be measured as a function of annealing temperatures and times.

Ion implantation has been one of the earliest subjects in computer calculations because of the relative simplicity of the collisional process. For this reason there are now computer codes capable of predicting quite accurately ion implantation range profiles in Si;⁵ these codes are based on the binary collision approximation (BCA), a repulsive interatomic potential and an electronic energy loss model. Ion implantation damage and its high temperature annealing, however, are far more complex problems than that of the range profile and certainly beyond the scope of binary collision codes. Molecular dynamics (MD) provides detailed predictions of the damage, but it can only be used to follow the evolution of the damage during the first nanoseconds be-

cause of its inherently heavy computational burden. These first stages obtained by MD simulation show that, instead of the Frenkel pairs generated by a BCA code, cascades in Si produce regions of high disorder plus some isolated point defects. However, MD simulations of high temperature anneals have shown⁶ that the damage regions collapse into vacancy and interstitial clusters and isolated point defects, which can all be simulated by the methods described below.

To help elucidate these processes we have developed an atomistic process simulator. This simulator (BLAST⁷) includes a Monte Carlo diffusion code coupled to a BCA program (MARLOWE⁸). The simulation is carried out in the following way. A cascade is developed by MARLOWE and the locations of vacancies and interstitials are passed on to the Monte Carlo diffusion simulator. Vacancies and interstitials are then given random jumps (at a rate derived from their diffusivities at that temperature), allowing for vacancy-interstitial recombination, clustering of like defects, re-emission from the clusters, and trapping and de-trapping of interstitials at native traps (e.g., carbon⁹). Annihilation occurs at the surface with a specified sink efficiency, and periodic boundary conditions are applied in the lateral direction. Diffusion proceeds until the arrival of a new cascade from MARLOWE, as determined by the implant dose rate. Successive cascades are generated and annealed until the implant dose is reached. An anneal is simulated by using the Monte Carlo diffusion simulator alone. A BLAST run takes around 10 hours on a typical workstation. The parameters used in the Monte Carlo simulation (Table I) were derived from MD calculations using the Stillinger-Weber potential for Si.⁶ The vacancy and intersti-

TABLE I. Cluster binding energies, in eV, for different cluster sizes (Ref. 6).

	2	3	4	5
Vac.	0.62	0.78	1.2	1.82
Int.	1.6	2.25	1.29	2.29

^{a)}Permanent address: Dept. de Electronica, Fac. de Ciencias, Univ. de Valladolid, 47011 Valladolid, Spain. Electronic mail: ghg@allwise.att.com

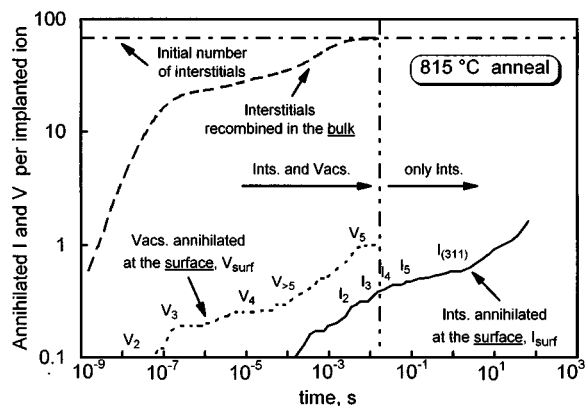


FIG. 1. Comparison between the number of interstitials recombined with vacancies in the bulk and the number of vacancies, V_{surf} , and of interstitials, I_{surf} , annihilated at the surface. The emission times for several cluster sizes are indicated as I_n , V_n .

tial diffusivities were $D_v = 0.001 \exp(-0.43/kT)$ and $D_i = 0.01 \exp(-0.9/kT)$ cm^2/s , respectively. The binding energy for infinitely large interstitial clusters [around 2 eV from MD calculations for (311) structures¹⁰] was set equal to 2.1 eV to match the 311' experimental decay.⁴ The binding energies for interstitial clusters with n interstitials were calculated from $E_{\text{bi}}(n) = 2.1 - 1.45(\sqrt{n} - \sqrt{n-1})$, which is a smoothed fit to the data in Table I, and approaches 2.1 eV as n becomes large. Similarly, vacancy cluster binding energies were obtained from $E_{\text{bv}}(n) = 3.65 - 5.15[n^{2/3} - (n-1)^{2/3}]$. Clusters and traps are assumed to be immobile. The trap activation energy is set to 3.5 eV and the trap concentration to $1.5 \times 10^{17} \text{ cm}^{-3}$.⁹ The jump distance¹¹ and capture radius were chosen equal to the second nearest neighbor distance in Si.

The simulation of a typical room-temperature implant of 40 keV, $5 \times 10^{13} \text{ cm}^{-2}$ Si into (001)Si, 7° tilt, yields a damage distribution consisting of small clusters of interstitials and vacancies. At the time (50 s) the implant has reached the final dose a fraction of the interstitial population is still free, although all of the vacancies are already in clusters due to their higher diffusivities. These free interstitials can still move at room temperature until they either form clusters or annihilate. We simulated a post-implant anneal and found that this transient takes three hours at room temperature. During this anneal, the number of interstitials per implanted ion decreases from 110 to 70. The depth distributions of interstitials and vacancies resemble those obtained using MARLOWE, only attenuated due to room-temperature recombination (~ 70 surviving interstitials per implanted ion, as compared to ~ 520 generated by MARLOWE).

For a subsequent anneal at 815 °C, for example, free vacancies are first emitted from their clusters, while the more tightly bound interstitials remain immobile in their small clusters. The free vacancies diffuse and annihilate most of the interstitials. Although the dominant annihilation process is recombination, some vacancies reach the surface (assumed to be a perfect sink) and annihilate there, leaving an excess of interstitials. Figure 1 shows the cumulative number of

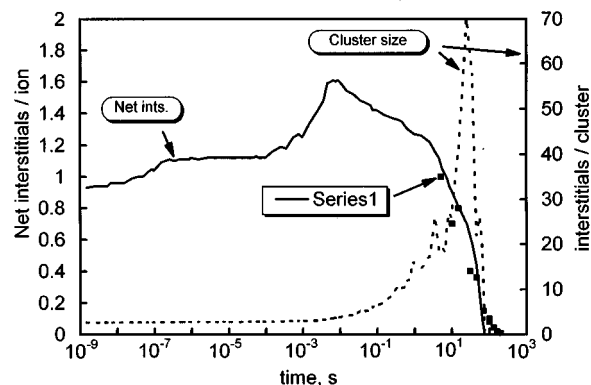


FIG. 2. Net excess of interstitials per implanted ion during the 815 °C anneal. The squares represent experimental data from TEM measurements of (311) defects (Ref. 4). Also shown is the average interstitial cluster size (dashed line).

vacancies (V_{surf}) and of interstitials (I_{surf}) annihilated at the surface, per implanted ion, as a function of time. The emission time constants for several cluster sizes, according to the parameter values used in the simulation, are also indicated as I_n , V_n . The emission from the vacancy clusters can be easily identified as an increase in V_{surf} , especially after 10^{-4} s, when the larger clusters break up. The increase in I_{surf} at the same time (before the interstitial clusters begin to evaporate) is due to free vacancies partially annihilating small interstitial clusters, and thus, releasing free interstitials. After 1 s all of the vacancies have disappeared. They are lost primarily by recombination with interstitials; only 1% of the vacancies diffuse to the surface.

Figure 2 plots the net excess of interstitials (interstitials minus vacancies) per implanted ion, throughout the anneal. The starting value (0.9) corresponds to the situation after the room temperature implant, and includes the contribution of the implanted ion (+1), the sputtered Si atoms (-0.3) and the surface contribution (+0.2) due to the fact that vacancies diffuse faster than interstitials and are slightly closer to the surface. The number of interstitials remaining when all the vacancies have disappeared is 1.4 per implanted ion, in agreement with recent TEM measurements.⁴ It is quite remarkable that the full blown calculation, with the sputtering and surface terms, gives such good confirmation of the “+1” model.

The depth distribution of the remaining interstitials is peaked at approximately twice the implant range because of the momentum transfer from the implant and the profile distortion due to interstitial annihilation at the surface. On annealing, the interstitial clusters undergo an Ostwald ripening process (Fig. 2, dashed line). These clusters have been seen at 815 °C and identified as the (311) defects.⁴ Eventually, the large clusters dissolve emitting interstitials that annihilate at the surface. The ripening of the interstitial clusters is sensitive to the precise values used for the binding energies of the interstitials to the clusters. In particular, if the actual binding energies in Table I are employed for clusters of two to five atoms instead of the smoothed analytical expression, then the growth of large clusters is inhibited by the slow evaporation

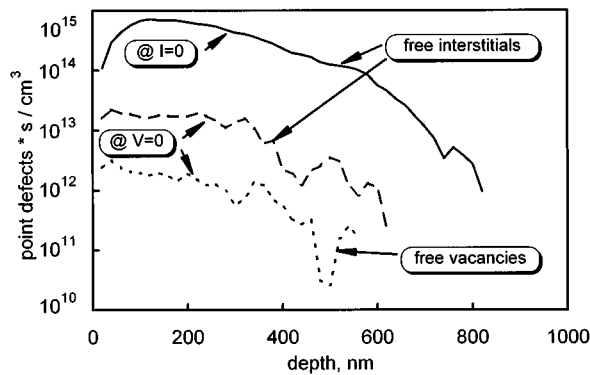


FIG. 3. Time integrated free I and V distributions after IV recombination ($V=0$) and after completion of TED ($I=0$). Most TED takes place after $T=0$, as implicitly assumed in the “+1” model.

from three and five atom interstitial clusters. The effect of traps is almost negligible because of their low concentration relative to that of the implanted ions.

We can conclude that the dominant process during the high temperature anneal is recombination. Consequently, the extra interstitials corresponding to the implanted ions (the “+1” model) make a major contribution to the excess interstitials. This was confirmed by a simulation where the implanted ion was deleted at the start of the diffusion process. In that case the simulation yields +0.5, as opposed to +1.4, directly reflecting the loss of the implanted ion. The clustering of interstitials only affects the time scale required to eliminate the interstitial excess during annealing. This was also confirmed by an annealing simulation without clusters ($E_{\text{bind}}=0$ for all clusters). In this case the vacancies disappear in 5×10^{-6} s leaving +1.3 interstitials per implanted ion. The “+1” model is, therefore, physically plausible because of the dominant role of bulk recombination, with only minor deviations due to sputtering, surface annihilation, and clustering. This feature makes it a particularly robust approximation, only weakly sensitive to changes in the implant or anneal parameters.

Finally, we can assess the implications of these results for dopant diffusion (TED). A close correlation between the excess interstitials and the induced TED can be drawn from

the free interstitial distribution, time-integrated throughout the anneal. Figure 3 shows this distribution both when the vacancies disappear ($V=0$) and after running TED to completion ($I=0$, annihilation of all the interstitials). We can conclude that most of the TED occurs after $V=0$. This explains why the continuum simulators yield good predictions using the “+1” model in this regime. However, we have simulated implants at doses as low as $5 \times 10^9 \text{ cm}^{-2}$ and then most of the TED takes place before $V=0$. This occurs because of the dilute I, V populations, where the probability of an I interacting with the dopant is greater than with a V . The use of the “+1” model in that regime would, consequently, underestimate the resulting TED. Also shown in Fig. 3 is the total time-integrated free vacancy distribution. The lower concentration of this distribution suggests an explanation for the lack of vacancy-mediated TED of Sb after implantation.⁹

In summary, the atomistic simulation of a Si implant and anneal provides, for the first time, a complete history of the I and V populations, including the formation and ripening of defect clusters. Besides revealing the mechanisms leading to the success of the “+1” model, it makes quantitative predictions on the contribution of each of those mechanisms and the limits of applicability of the “+1” approximation.

We acknowledge stimulating discussions with D. J. Eaglesham, C. S. Rafferty, and P. A. Stolk. One of us (M.J.) acknowledges partial financial support from DGICYT, Espana.

¹ SUPREM-IV developed at the Integrated Circuit Lab, Stanford University, by R. W. Dutton and J. D. Plummer.

² M. R. Pinto, D. M. Boulton, C. S. Rafferty, R. K. Smith, W. M. Coughran, Jr., I. C. Kizilyalli, and M. J. Thoma, IEDM Tech. Dig., 923 (1992).

³ M. D. Giles, J. Electrochem. Soc. **138**, 1160 (1991).

⁴ D. J. Eaglesham, P. A. Stolk, H.-J. Gossmann, and J. M. Poate, Appl. Phys. Lett. **65**, 2305 (1994).

⁵ K. M. Klein, C. Park, and A. F. Tasch, Nucl. Instrum. Methods B **59/60**, 60 (1991).

⁶ G. H. Gilmer, T. Diaz de la Rubia, D. M. Stock, and M. Jaraiz, Nucl. Instrum. Methods B **102**, 247 (1995).

⁷ M. Jaraiz, G. H. Gilmer, T. D. de la Rubia, and J. M. Poate (unpublished).

⁸ M. T. Robinson and I. M. Torrens, Phys. Rev. B **9**, 5008 (1974).

⁹ P. A. Stolk, D. J. Eaglesham, H.-J. Gossmann, and J. M. Poate, Appl. Phys. Lett. **66**, 568 (1995); Nucl. Instrum. Methods B **96**, 187 (1995).

¹⁰ M. Kohyama and S. Takeda, Phys. Rev. B **51**, 13111 (1995).

¹¹ K.-H. Heinig (private communication).